

Meyer, E. et al. (2016) Mutations in the histone methyltransferase gene KMT2B cause complex early-onset dystonia. *Nature Genetics*, 49(2), pp. 223-237. (doi:[10.1038/ng.3740](https://doi.org/10.1038/ng.3740))

This is the author's final accepted version.

There may be differences between this version and the published version. You are advised to consult the publisher's version if you wish to cite from it.

<http://eprints.gla.ac.uk/169390/>

Deposited on: 21 September 2018

Enlighten – Research publications by members of the University of Glasgow
<http://eprints.gla.ac.uk>

Mutations in the Histone Methyltransferase Gene, *KMT2B* Cause Early Onset Dystonia

¹Meyer E[^], ^{2,3}Carss KJ[^], ⁴Rankin J[^], ⁵Nichols J, ^{6,7}Grozeva D, ⁸Joseph AP, ⁹Mencacci NE, ^{1,10}Papandreou A, ^{1,10}Ng J, ¹Barral S, ^{1,10}Ngoh A, ¹¹Ben-Pazi H, ¹²Willemsen MA, ¹³Arkadir D, ¹⁴Barnicoat A, ¹⁵Bergman H, ¹⁰Bhate S, ¹⁶Boys A, ¹⁷Darin N, ¹⁸Foulds N, ¹⁹Gutowski N, ²⁰Hills A, ⁹Houlden H, ¹⁴Hurst J, ²¹Israel Z, ²²Kaminska M, ²³Limousin P, ²²Lumsden D, ²⁴McKee S, ^{25,26}Misra S, ^{25,26}Mohammed SS, ²²Nakou V, ²⁷Nicolai J, ²⁸Nilsson M, ²⁹Pall H, ³⁰Peall KJ, ³¹Peters GB, ¹⁰Prabhakar P, ³²Reuter MS, ³³Rump P, ³⁴Segel R, ²⁷Sinnema M, ³⁵Smith M, ⁴Turnpenny P, ¹⁵White S, ³⁶Wieczorek D, ²⁰Wilson B, ¹⁴Winter G, ¹⁹Wragg C, ³⁷Pope S, ^{37,38}Heales SJH, ³⁹Morrogh D, ⁷The UK10K Consortium, ⁴⁰DDD study, ³NIHR Bioresource Rare Diseases Consortium, ⁹Pittman A, ¹⁰Carr LJ, ^{41,42}Perez-Dueñas B, ²²Lin JP, ³²Reis A, ⁴³Gahl WA, ⁴³Toro C, ^{9,23}Bhatia KB, ^{9,23}Wood NW, ⁴⁴Kamsteeg EJ, ⁴⁵Chong WK, ⁵Gissen P, ⁸Topf M, ^{25,26}Dale RC, ⁵Chubb JR, ^{3,6,7}Raymond FL⁺, ^{1,10}Kurian MA⁺*

[^]These authors contributed equally

⁺These authors contributed equally

*Corresponding author: **Dr Manju Kurian** (manju.kurian@ucl.ac.uk)

Affiliations:

1. Molecular Neurosciences, Developmental Neurosciences, UCL-Institute of Child Health, London, UK

2. Department of Haematology, University of Cambridge, NHS Blood and Transplant Centre, Cambridge, UK
3. NIHR Bioresource Rare Diseases, University of Cambridge, Cambridge, UK
4. Clinical Genetics, Royal Devon & Exeter Hospital, Exeter, UK
5. MRC Laboratory for Molecular Cell Biology, UCL, London, UK
6. Department of Medical Genetics, Cambridge Institute for Medical Research, University of Cambridge, Cambridge, UK
7. Wellcome Trust Sanger Institute, Hinxton, Cambridge, UK
8. Institute of Structural and Molecular Biology, Crystallography/Department of Biological Sciences, Birkbeck College, University of London, London, UK
9. Department of Molecular Neuroscience, UCL-Institute of Neurology, London, UK
10. Department of Neurology, Great Ormond Street Hospital, London, UK
11. Pediatric Neurology and Development, Shaare-Zedek Hospital, Jerusalem, Israel
12. Department of Paediatric Neurology, Donders Centre for Brain, Cognition, and Behavior, Radboud University Medical Center, Nijmegen, Netherlands
13. Department of Neurology, Hadassah Medical Center and the Hebrew University, Jerusalem, Israel
14. Department of Clinical Genetics, Great Ormond Street Hospital, London, UK
15. Department of Neurobiology and Neurosurgery, The Hebrew University, Hadassah Medical Centre, Jerusalem, Israel
16. Victoria Clinical Genetics Services, Murdoch Children's Research Institute, Parkville, Victoria, Australia

-
- 51 17. Department of Neurology, The Queen Silvia Children's Hospital,
52 Sahlgrenska University Hospital, Gothenburg, Sweden
- 53 18. Department of Clinical Genetics, Southampton General Hospital,
54 Southampton, UK
- 55 19. Department of Neurology, Royal Devon and Exeter NHS Foundation Trust,
56 Exeter, UK
- 57 20. Bristol Genetics Laboratory, Bristol, UK
- 58 21. Functional and Restorative Neurosurgery, Hadassah University Hospital,
59 Jerusalem, Israel
- 60 22. Complex Motor Disorders Service, Evelina Children's Hospital, Guy's & St
61 Thomas' NHS Foundation Trust, London, UK
- 62 23. Sobell Department of Motor Neuroscience and Movement Disorders,
63 National Hospital for Neurology and Neurosurgery, London, UK
- 64 24. Northern Ireland Regional Genetics Service, Belfast City Hospital, Belfast,
65 UK
- 66 25. Child and Adolescent Health, University of Sydney, Sydney, Australia
- 67 26. Institute for Neuroscience and Muscle Research, The Children's Hospital at
68 Westmead, University of Sydney, Sydney, Australia
- 69 27. Department of Neurology, Maastricht University Medical Center, Netherlands
- 70 28. Department of Pediatrics, Piteå Hospital & Umeå University Hospital,
71 Sweden
- 72 29. College of Medicine and Dental Studies, The University of Birmingham,
73 Birmingham, UK

-
- 74 30. Neuroscience and Mental Health Research Institute, Institute of
75 Psychological Medicine and Clinical Neurosciences, Cardiff University,
76 Cardiff, UK
- 77 31. Department of Cytogenetics, The Children's Hospital at Westmead,
78 Westmead, Australia
- 79 32. Institute of Human Genetics, Friedrich-Alexander-Universität Erlangen-
80 Nürnberg, Erlangen, Germany
- 81 33. Department of Genetics, University of Groningen, University Medical Center
82 Groningen, Netherlands
- 83 34. Medical Genetics Institute and Pediatrics, Shaare Zedek Medical Center and
84 the Hebrew University School of Medicine, Jerusalem, Israel
- 85 35. Department of Paediatric Neurology, John Radcliffe Hospital, Oxford, UK
- 86 36. Institute of Human Genetics, University Duisburg-Essen, Essen, Germany
- 87 37. Neurometabolic Unit, National Hospital for Neurology and Neurosurgery,
88 Queen Square, London, UK
- 89 38. Clinical Chemistry, Great Ormond Street Children's Hospital, NHS
90 Foundation Trust, London, UK
- 91 39. North East Thames Regional Genetics Service, Great Ormond Street
92 Hospital, London, UK
- 93 40. DDD Study, Wellcome Trust Sanger Institute, Hinxton, Cambridge, UK
- 94 41. Department of Child Neurology, Hospital Sant Joan de Déu, Universitat de
95 Barcelona, Barcelona, Spain
- 96 42. Centre for Biomedical Research in Rare Diseases (CIBERER-ISCIII),
97 Hospital Sant Joan de Déu, Barcelona, Spain
- 98 43. NIH Undiagnosed Diseases Program, Common Fund, Office of the Director,

- 99 National Institutes of Health, Bethesda, Maryland, USA
- 100 44. Department of Human Genetics, Radboud University Medical Center,
- 101 Nijmegen, Netherlands
- 102 45. Department of Radiology, Great Ormond Street Hospital, London, UK

ABSTRACT

Histone lysine methylation mediated by mixed-lineage leukemia (MLL) proteins, has emerged as critical in the regulation of gene expression, genomic stability, cell cycle and nuclear architecture. Although postulated to be essential for normal development, little is known about the specific functions of the different MLL lysine methyltransferases. Here, we report heterozygous mutations in *KMT2B* (*MLL4*) in 27 unrelated individuals with a complex progressive childhood-onset dystonia, often associated with a typical facial appearance and characteristic findings on brain magnetic resonance imaging. Over time the majority developed prominent cervical, cranial and laryngeal dystonia. Marked clinical benefit was observed following deep brain stimulation (DBS), leading to even restoration of independent ambulation in some cases. Decreased gene expression of *THAP1* and *TOR1A* was evident in cultured skin fibroblasts from subjects with *KMT2B* mutations, with reduced THAP1 protein levels on immunoblotting. Analysis of cerebrospinal fluid from *KMT2B* mutation-positive patients revealed markedly reduced levels of dopamine 2 receptor protein, with increased tyrosine hydroxylase levels. Our findings highlight a major new, clinically recognizable, and potentially treatable form of genetic dystonia, demonstrating the crucial role of KMT2B in the physiological control of voluntary movement.

122

123 **INTRODUCTION**

124 The control of voluntary movement is governed by interactive neural networks
125 within the brain, involving the basal ganglia, sensorimotor cortex, cerebellum and
126 thalamus¹. Disruption of such pathways can lead to the development of a variety of
127 motor disorders. Dystonia is one such movement disorder characterized by
128 sustained or intermittent muscle contractions, causing abnormal, often repetitive
129 movements and postures affecting the limbs, trunk, neck and face. Dystonic
130 movements are typically patterned, twisting, and may be tremulous, often initiated
131 or worsened by voluntary action and associated with overflow muscle activation².

132 Dystonia is the 3rd most commonly reported movement disorder worldwide¹. It is
133 described in a broad spectrum of genetic and acquired disorders, either in isolation
134 or combined with other neurological and systemic features². The precise
135 pathophysiological processes remain yet to be fully elucidated, but defective
136 dopaminergic signaling is thought to play an important role in many forms of
137 isolated and complex dystonia^{1,3-5}.

138 Despite genetic advances, the underlying cause remains elusive for a significant
139 proportion of individuals with childhood-onset dystonia, hindering future
140 prognostication and treatment strategies⁶. Here we report 27 individuals with an
141 early-onset, complex, combined progressive dystonia associated with mono-allelic
142 mutations in *KMT2B* (*MLL4*, OMIM *606834). *KMT2B* encodes a lysine histone
143 methyltransferase, involved in H3K4 methylation, an important epigenetic
144 modification associated with active gene transcription.

145

146 **RESULTS**

147 ***Chromosomal microdeletions and intragenic KMT2B mutations in early-onset*** 148 ***dystonia***

149 We identified a cohort of 34 patients with undiagnosed childhood-onset dystonia for
150 further molecular genetic investigation ([**Online Methods, Supplementary Table 1,**
151 **Supplementary Fig. 1**). On routine diagnostic testing, one case (Patient 1) was
152 found to have a microdeletion at 19q13.12 of undetermined significance⁷.
153 Diagnostic chromosomal microarray was therefore undertaken in as many patients
154 as logistically possible from this cohort (n=20) and overlapping microdeletions were
155 detected in 5 more children (**Supplementary Table 1**, Patients 2-6). Using
156 established networks (**Online Methods, Supplementary Fig. 1**), 4 more cases
157 (Patients 7-10) with microdeletions were identified. In total, 10 patients (Patients 1-
158 10) were found to have overlapping heterozygous interstitial microdeletions at
159 19q13.11-19q13.12 (**Table 1a, Fig.1**). Deletions detected on diagnostic microarray
160 studies were confirmed by standard established laboratory protocols and confirmed
161 *de novo* where parental testing was possible (**Supplementary Table 2a**). The
162 smallest region of overlap extended from 36,191,100-36,229,548bp
163 (GRCh37/Hg19), and contained two HUGO Gene Nomenclature Committee
164 curated genes, *ZBTB32* (zinc finger and BTB domain containing 32) and *KMT2B*
165 (*MLL4*) (**Fig. 1**).

166 Of the remaining 28 patients from the original cohort, we undertook research exome
167 (n=6) and genome sequencing (n=9) in 15 patients (**Online Methods**).
168 Heterozygous variants of *KMT2B* were identified in 6/15 cases (Patients 13, 14, 17,

21, 22, 27). Subsequent Sanger sequencing of *KMT2B* in the other 13/28 individuals from the original cohort detected one more mutation-positive case (Patient 16). A further 10 cases (Patients 11, 12, 15, 18, 19, 20, 23, 24, 25, 26a) were ascertained through both national and international collaborators (**Online Methods, Supplementary Fig. 1**). In total, 17 patients with intragenic heterozygous *KMT2B* variants were identified, harboring frameshift insertions (n=1), frameshift deletions (n=6), splice site (n=1), stop-gain (n=2) and missense (n=7) mutations (**Fig.1**). All *KMT2B* mutations were confirmed on Sanger sequencing and parental segregation studies completed where DNA was available (**Table 1a, Fig. 1, Supplementary Table 2a, Supplementary Fig. 2**). No pathogenic variants in either *ZBTB32* or other known disease-associated genes (including genes causing clinically similar forms of dystonia) were otherwise identified in patients who had whole exome or genome sequencing. In the remaining patients, where further genetic testing was possible, mutations in *TOR1A*, *THAP1* and *GNAL* were excluded by diagnostic single gene testing, multiple gene panel testing or research Sanger sequencing (**Supplementary Table 3**).

Phenotypic characterization of patients with KMT2B mutations

Overall, we identified 27 patients (current age 6-40 years, 14 female, 13 male) with childhood-onset progressive dystonia (**Table 1a, Table 1b, Supplementary Table 4, Supplementary Videos 1-7**). Individuals presented in early childhood (1-9 years, median age 4 years) with either limb or cranio-cervical dystonia. Clinical presentation for those with microdeletions, frameshift, splice-site and stop-gain variants (mean age 4.1 years) occurred significantly earlier than for those with intragenic missense mutations (mean age 6.4 years) (p-value 0.0223)

(**Supplementary Fig. 3a**). Most patients (21/27) had lower limb symptoms at disease onset, leading to foot posturing, toe-walking and gait disturbance (**Fig. 2a**). 4/27 patients presented initially with upper limb symptoms associated with abnormal postures (**Fig. 2b,c**) and dystonic tremor, leading to reduced dexterity and handwriting difficulties (**Supplementary Fig. 4a,b**). With increasing age, cervical symptoms (torticollis, retrocollis) (**Fig. 2d,e**) and cranial involvement (facial dystonia, oromandibular involvement with dysarthria/anarthria and difficulties in chewing/swallowing) became prominent features in the majority of patients. In many patients, progressively severe dysphonia was suggestive of laryngeal involvement. None of the patients had airway compromise and videostroboscopy was not undertaken. Over time, the majority of patients (24/27) developed progressive generalized dystonia, 2-11 years after initial presentation (**Fig. 2f**). The dystonia was persistent in nature, absent in sleep, worsened by voluntary action and associated with overflow muscle activation. Some patients had dystonic tremor. Sudden, brief, involuntary muscle jerks, clinically consistent with myoclonus was evident in 2 cases (Patients 14 and 27). For a few subjects, dystonia was exacerbated when systemically unwell. Stepwise deterioration following intercurrent illness was particularly evident in Patient 14, and status dystonicus, triggered by a urinary tract infection, was reported in Patient 3.

Many patients with *KMT2B* mutations had further clinical findings. Additional neurological symptoms and signs were evident in some patients, including microcephaly, seizures, spasticity and eye movement abnormalities (strabismus, saccade initiation failure and oculomotor apraxia) (**Table 1b**). Dysmorphic features and characteristic facial appearance (elongated face and bulbous nasal tip) (**Fig. 2g, Table 1b**) were commonly reported. Delay in neurodevelopmental milestones,

intellectual disability, systemic (dermatological, renal, respiratory) features and psychiatric symptoms were also present in some individuals (**Table 1b**, **Supplementary Table 4**, **Supplementary Fig. 4c**). Malignancies were not reported in any patients. Cerebrospinal fluid (CSF) neurotransmitter analysis was undertaken in 13 patients revealing no major derangement of monoamine metabolites (**Supplementary Table 5a**). Magnetic resonance (MR) imaging revealed a characteristic signature in 17/22 patients who had imaging sequences suitable for assessment (**Supplementary Table 5b**). Subtle symmetrical hypointensity of the globus pallidi (with a hypointense streak of bilateral globus pallidus externa) was evident on MR images known to be sensitive to the magnetic resonance phenomenon of susceptibility (T2^{*}-, susceptibility- and echo-planar imaging b0-diffusion-imaging datasets) (**Fig. 3**). The mean age at neuroimaging was significantly lower for patients with MR abnormalities (11.7 years) than for those with normal brain scans (19.0 years) (p-value 0.0167) (**Supplementary Fig. 3b**). Single positron emission tomography using ¹²³I (DaTSCAN™) and 18 FDG-PET-CT glucose uptake studies, each undertaken in 3 patients, were normal (**Supplementary Table 5b**, **Supplementary Fig. 4d**).

Deep brain stimulation: clinical benefit in KMT2B-dystonia

Overall, medical therapies were not of clinical benefit in this patient cohort. None of the patients had a sustained response to levodopa treatment, nor other commonly used anti-dystonic agents (**Table 1a**). Due to the medically intractable, progressive nature of disease, 10 patients had symptomatic treatment with bilateral globus pallidus interna-deep brain stimulation (GPi-DBS) (**Table 1a**). All showed clinical benefit with DBS (which was particularly striking in some of the younger patients)

with overall amelioration of dystonia, improved oromandibular symptoms, better upper and lower limb function and even restoration of independent ambulation in some patients. Patient 6 showed significant improvement of torticollis and retrocollis, as well as in overall function and gait after DBS. Patient 8 showed a sustained clinical response 6 years after DBS insertion, with improvement of dystonia, even more evident after replacement of a faulty right DBS lead. Patient 9 had generalized dystonia and could not walk independently pre-DBS. Two weeks post-DBS insertion he dramatically regained independent ambulation with marked improvement of dystonic symptoms (**Supplementary Video 8**). Patient 17 and 21 were predominantly wheelchair-dependent pre-DBS insertion, but both patients showed restoration of independent walking and improvement of dystonia after DBS (**Supplementary Video 9,10**). Patient 19 had improvement in oromandibular symptoms with DBS. Patient 20 had DBS insertion at age 32 years and although most benefits were only transient, sustained improvement of foot posture was reported. Patient 23 had significant amelioration of dystonia symptoms after DBS insertion. Patient 22, now 9 months post-DBS (**Supplementary Video 11**) and Patient 25, 4 months post-DBS have both shown significant gains in hand function and independent walking with reduction of dystonia. Five patients in the cohort are now over three years post-surgery, and the observed reduction of dystonia, restoration of function and prevention of progressive disability is evidence of sustained clinical benefit.

KMT2B is constrained for missense and predicted protein truncating variants

Four individuals (Patient 13, 14, 17 and 21) had whole genome sequencing as part of the NIHR-funded BioResource-Rare Disease project. Enrichment analysis was undertaken in this cohort in order to determine whether predicted protein truncating

variants (PPTVs) in *KMT2B* are observed more frequently in patients than would be expected by chance. Given the size and sequence context of *KMT2B*, 5.73×10^{-03} *de novo* PPTVs are expected to occur by chance in *KMT2B* in the subset of the NIH BioResource- Rare Diseases cohort who have pediatric onset neurological disease, but 3 PPTVs are observed. This represents a significant enrichment (p-value 3.12×10^{-08}). Furthermore in ExAC, *KMT2B* is also highly constrained for PPTVs. In the ExAC database of 60,706 individuals (Exome Aggregation Consortium (ExAC), Cambridge, MA (URL: <http://exac.broadinstitute.org>, accessed July 2016)⁸, there are only 5 PPTVs that are not flagged as having dubious variant annotation. All are extremely rare (4 are found in a single individual and one occurs in 2 individuals). Given the size and sequence context of the gene, the presence of so few PPTVs in a cohort of 60,706 individuals reveals *KMT2B* to be highly constrained for such variation, providing supportive evidence of its pathogenicity. Regarding variants in the ExAC database, there are 712 reported non-synonymous changes. Most of these are rare, as expected for a cohort of this size, and the median CADD score⁹ for these variants is 22.9. The median CADD score for missense mutations identified in our *KMT2B*-dystonia cohort is significantly higher at 29.1 (p-value 0.0001364; **Supplementary Table 2b**). Furthermore, given the size and sequence context of *KMT2B*, 956 missense variants are predicted to occur by chance, suggesting that *KMT2B* may also be constrained for missense variation ($z=4.06$)⁸.

***KMT2B* variants are predicted to destabilize protein structure**

In silico homology modelling studies were undertaken to generate hypotheses regarding the predicted effects of mutations on *KMT2B* structure-function properties (**Supplementary Results**). Based on Pfam domain assignments, *KMT2B* has a

291 CXXC zinc finger domain, multiple PHD domains, an F/Y rich N-terminus (FYRN),
292 FYRC (F/Y rich N-terminus) domain and a C-terminal SET domain (**Fig. 4a**). The
293 modelled mutations occurred in residues within the PHD-like, FYRN, SET and
294 FYRC-SET linking domains (**Fig. 4b-d**). Evaluation of a number of mutations using
295 MAESTRO¹⁰ and DUET¹¹ suggests change in free energy, with a predicted
296 structure destabilizing effect (**Supplementary Results**).

297 Mutations Phe1662Leu and Gly1652Asp occur within a PHD-like domain (residues
298 1574-1688), predicted to facilitate interaction with DNA, protein-protein interaction
299 and recognition of methylated/unmethylated lysines¹²⁻¹⁴. Extensive hydrophobic
300 interactions hold the globular structure of this region, which is important for its
301 function¹². Phe1662 is fully buried at the core, stabilizing the structure of this PHD-
302 like domain while Gly1652 is partially buried (**Fig. 4b,e,f**). Phe1662 is involved in
303 multiple hydrophobic contacts at the core of the PHD domain, and mutation to
304 leucine is predicted to cause loss of contacts at the core (**Fig. 4g**). Gly1652 is
305 located on a loop (**Fig. 4e**) and mutation to aspartic acid is predicted to alter surface
306 charge, with possible effect on the interaction network in the vicinity, involving a
307 positively charged Arg1635, part of the helix $\alpha 3$ implicated in DNA binding¹².
308 Arg1762 and Leu1781 occur in a FYRN domain. FYRN and FYRC regions,
309 particularly common in MLL histone methyltransferases, interact to form a compact
310 structural unit (**Fig. 4c,h**), important in maintaining the active structure^{15,16}. Arg1762
311 forms hydrogen bonds with the backbone carboxyls of Arg2463 and Leu2464 of
312 FYRC domain. Substitution of Arg1762 by cysteine is predicted to abolish these
313 contacts and hence contribute to destabilization of FYRC-FYRN association.
314 Leu1781, at the interface between FYRN and FYRC (**Fig. 4h,i**) is surface exposed
315 and involved in backbone hydrogen bonds stabilizing the beta sheet formed

together by the two domains. Mutation to proline is predicted to disrupt the backbone hydrogen bond at this position, because it lacks one hydrogen bond donor and its backbone torsion angles are not compatible with that of a beta sheet, with a predicted destabilizing effect on sheet structure, potentially affecting the normal association of FYRN and FYRC domains. Arg2517 resides in the region linking FYRC and SET domains, known to bind WDR5, an effector required for trimethylation of histone H3¹⁷, presenting methylated histone H3 substrates to the MLL complex for further methylation¹⁸. Arg2517 is thought to be involved in a salt-bridge interaction with Asp172 of WDR5 (**Fig. 4j**) and Arg2517Trp is predicted to lead to loss of this interaction. Ile2674, Tyr2688 and Ile2694 occur in the catalytic methyltransferase SET domain common to histone lysine methyltransferases. Ile2674 is buried in the hydrophobic core, adjacent to the catalytic site (**Fig. 4d,k**). Mutation to threonine is predicted to lead to loss of contacts at the core of the domain (due to the shorter side chain) and also introduces a buried polar group (**Fig. 4k,l**). Tyr2688Thr occurs at the core of SET domain involving extensive hydrophobic interactions and a hydrogen bond interaction with Ser2661 (**Fig 4m**). The frameshift mutation Tyr2688Thrfs*50 with insertion of 50 additional residues, is predicted to destabilise the core and affect contacts due to the substitution with a shorter non-aromatic side-chain. Ile2694 is involved in the extensive hydrophobic contacts stabilizing the core of this domain. *In silico* analysis predicts that the frameshift mutation Ile2694Serfs*44 will disrupt the domain fold and affect methyltransferase activity.

KMT2B is ubiquitously expressed with reduced expression in KMT2B-dystonia

We confirmed widespread *KMT2B* expression in a variety of control fetal and adult human tissues (**Fig. 5a**). Moreover, *KMT2B* is ubiquitously expressed in the brain, with higher expression in the cerebellum than any other region (**Fig. 5b**). We ascertained fibroblasts from 4 patients (Patient 2, 13, 14, 16, with either microdeletions or PPTVs in *KMT2B*) and detected a statistically significant decrease in fibroblast *KMT2B* expression on quantitative RT-PCR when compared to control fibroblasts (**Fig. 5c**).

Histone H3K4 methylation is not globally reduced in KMT2B-dystonia

To determine the effect of *KMT2B* mutations on methylation of lysine 4 on histone H3 (H3K4 methylation), we assayed tri-methylated H3K4 (H3K4me3) and di-methylated H3K4 (H3K4me2). Immunoblotting of histones extracted from fibroblasts of Patient 14 and 16 showed no significant reduction in H3K4me3 or H3K4me2 relative to control samples (**Fig. 5d, Supplementary Fig. S5a**). We used the model species *Dictyostelium discoideum* to test the effect of SET domain mutation Ile2647Thr on *in vivo* histone methyltransferase activity. The SET domain of *KMT2B* shares 56% sequence identity with the *Dictyostelium* orthologue DdSet1, and Ile2647 is conserved (corresponding amino acid in *Dictyostelium* is Ile1447) (**Fig. 1h**). DdSet1 is the only H3K4 methyltransferase in *Dictyostelium* and targeted knockout of *DdSet1* (*set1*⁻) results in loss of all methylation at H3K4¹⁹. We constitutively expressed wild-type DdSet1 (WT-DdSet1) and mutant-DdSet1 (m-DdSet1), both with N-terminal GFP fusions, in *set1*⁻ *Dictyostelium* cells and compared the resulting levels of H3K4 methylation. Expression of either GFP-WT-DdSet1 or GFP-mDdSet1 in *set1*⁻ cells resulted in rescue of H3K4 tri-methylation to wild type levels (**Fig. 5e, Supplementary Fig. S5b, S5c**).

Fibroblast THAP1 gene and protein expression is reduced in KMT2B-dystonia

In order to determine whether KMT2B-dystonia is associated with dysregulation of specific genes implicated in the control of movement, we investigated the expression profiles of *TOR1A* and *THAP1*. Fibroblasts derived from 4 patients (Patients 2, 13, 14, 16) showed significantly reduced transcript levels of *THAP1* and *TOR1A* when compared to control fibroblasts (**Fig. 5f**). Fibroblast immunoblotting studies showed a statistically significant reduction in THAP1 protein expression in all 4 patients when compared to control samples (**Fig. 5g**). A statistically significant reduction in TOR1A protein level was evident in Patient 14, though not in the other patients (**Fig. 5h**).

Abnormal CSF levels of dopaminergic proteins in KMT2B-dystonia

CSF immunoblotting studies were undertaken in two patients for whom samples were available for research testing (Patient 2 and 16). Both patients had markedly reduced levels of dopamine 2 receptor (D2R), 56.9% and 59.8% of levels observed in control CSF (Controls = 1.09 ± 0.21 SD, KMT2B patients = 0.64 ± 0.02 SD). In contrast, an increase in tyrosine hydroxylase (TH) levels was seen in both mutation-positive patients (173.3% and 170.9% of levels seen in control CSF) (Controls = 0.52 ± 0.08 SD, KMT2B patients = 0.90 ± 0.01 SD) (**Fig. 5i**).

DISCUSSION

We report 27 individuals with heterozygous mutations in the lysine methyltransferase gene, *KMT2B*, and define a new genetic movement disorder that importantly, is amenable to treatment with DBS. Using the current classification system², KMT2B-dystonia is defined as an inherited autosomal dominant, complex,

combined dystonia usually of infantile or childhood-onset. In most patients, the dystonia is persistent and progressive in nature. The majority of individuals develop 4-limb dystonia with particularly prominent cervical, laryngeal and oromandibular symptoms. Whilst the majority of patients in this cohort seem to follow this disease trajectory, we also report atypical cases with relatively little limb involvement and either mainly oromandibular features (Patient 18) or paroxysmal cervical dystonia (Patient 26a).

For many patients, KMT2B-dystonia is associated with a number of additional clinical features, including other neurological symptoms, intellectual disability, psychiatric co-morbidity, dysmorphia, skin lesions and other systemic signs. Given the association with active gene expression, is possible that *KMT2B* could account for these additional disease features. For Patients 1-10, is also possible that other genes within their microdeletion could contribute to aspects of their clinical phenotype. Indeed, cutis aplasia and ectodermal dysplasia have been reported in patients with more proximal deletions of chromosome 19q13.11²⁰. KMT2B is therefore a complex dystonia, and affected patients should have close surveillance of development during childhood, regular neurology assessments, routine dermatological review and formal neuropsychiatric testing.

In KMT2B-dystonia, the majority of patients had a characteristic pattern on MR imaging, with very subtle low pallidal signal on T2^{*}-, diffusion- and susceptibility-weighted sequences, particularly affecting the lateral aspect of the globus pallidus externa (**Fig. 3**). Although genotype did not appear to influence whether MR findings were evident, those with abnormal imaging had scans undertaken at a significantly younger age than those with normal imaging. Indeed, MR abnormalities could possibly be an age-dependent phenomenon, perhaps becoming less

apparent with increasing age, as was evident in Patient 22 (**Supplementary Table 5b, Supplementary Fig. 3b,c,d**). The overall significance of the identified neuroradiological abnormalities remains unclear. Such radiological findings are reminiscent of, but much more subtle and different to those reported in classical Neurodegeneration with Brain Iron Accumulation (NBIA) syndromes^{21,22}. Similar non-specific features of T2*-weighted hypointensity are increasingly recognized in a number of other neurological conditions, including Huntington's disease, *TUBB4A*-related disorders, GM1 gangliosidosis, alpha-fucosidosis and mitochondriocytopathies.

In the original UCL-ICH Dystonia cohort, *KMT2B* mutations were identified in 13/34 (38%) individuals with a relatively homogenous phenotype of early onset progressive dystonia. In other screened cohorts, mutation detection rates varied from 1.3-30%, with more cases identified from cohorts that were tightly phenotyped for dystonia (**Supplementary Fig. 1**). In screened cases where *KMT2B* mutations were not detected, it is likely that these individuals have another underlying etiology accounting for their symptoms, although it is possible that (i) single/multiple exon *KMT2B* deletions and duplications may have been missed on microarray, Sanger sequencing and whole exome/genome sequencing and (ii) promoter mutations and deeply intronic *KMT2B* variants may not have been detected by whole exome and Sanger sequencing.

The majority of individuals with *KMT2B* mutations (20/27, Patients 1-20) had either heterozygous interstitial microdeletions leading to *KMT2B* haploinsufficiency, or variants predicted to cause protein truncation, protein elongation, splicing defects or nonsense-mediated mRNA decay. The remaining 7 patients (Patients 21-27) had previously unreported non-synonymous variants of *KMT2B*, all affecting conserved

residues within key protein domains (**Fig. 1c-h**), and *in silico* studies predict destabilization of protein structure. Notably, initial disease presentation was significantly earlier in Patients 1-20 than in those with missense variants (**Supplementary Fig. 3a**). In KMT2B-dystonia, genotype did not however influence the rate of symptom evolution, disease severity or response to DBS.

For the majority of patients, *KMT2B* mutations were confirmed as *de novo* where parental testing could be undertaken. In our cohort, 3 patients had missense mutations that were all maternally inherited (Patient 22, 26a, 27). Given this observation of maternal inheritance, the possibility of imprinting at the disease locus was considered, but deemed unlikely, given (i) *de novo* microdeletions in Patients 2 and 10 occurred on paternally inherited alleles and (ii) there is evidence of bi-allelic expression of *KMT2B* single nucleotide polymorphisms in human tissues, including brain (**Supplementary Fig. S6**). Importantly, whole exome sequence analysis undertaken in Patients 22, 26a and 27 did not identify other rare or *de novo* variants to account for their disease. Interestingly, Patient 26a inherited p.Arg2517Trp from his symptomatic mother (26b) who also had (milder) disease symptoms. She reported gait abnormalities and a progressive inability to run, as well as periodic paroxysmal upper limb and neck dystonia. She also had a bulbous nasal tip, like her son (**Fig. 2g**). In contrast, both mothers of Patients 22 and 27 were clinically examined, and neither had evidence of a motor phenotype, intellectual disability, other neurological features, neuropsychiatric symptoms, facial dysmorphism, skin lesions or other systemic signs. The identification of both symptomatic and asymptomatic carriers suggests that there may be either ‘apparent’ incomplete penetrance, due to parental mosaicism, or true incomplete disease penetrance, a phenomenon commonly reported in a number of other autosomal dominant genetic

dystonias^{23,24}. Furthermore, other genetic, epigenetic and environmental modifiers may also influence disease penetrance and phenotypic presentation in KMT2B-dystonia.

KMT2B encodes an ubiquitously expressed lysine methyltransferase specifically involved in H3K4 methylation^{25,26}, an important epigenetic modification associated with active transcription. H3K4me3 is enriched at promoters, marking transcription start sites of actively transcribed genes, whereas H3K4me1 is associated with active enhancer sequences²⁷. H3K4me2 is less specifically localized, but may be enriched at transcription factor binding sites²⁸. Members of the SET/MLL protein family, including *KMT2B*, are responsible for the generation of H3K4me1, H3K4me2, and H3K4me3, essential for gene activation in normal development²⁹. Using patient-derived fibroblasts and a *Dictyostelium discoideum* model, we demonstrated that *KMT2B* mutations are not associated with widespread alterations in overall levels of H3K4 methylation. This is not surprising, given that haploinsufficiency of other MLL family members have not been convincingly shown to affect global H3K4 levels. The fundamental physiological role of MLL proteins is however further affirmed by the observation that loss-of-function heterozygous mutations in MLL-encoding genes are reported in human developmental disorders³⁰, namely Wiedemann Steiner (*KMT2A*, *MLL1*)³¹, Kleefstra-like (*KMT2C*, *MLL3*)³², Kabuki (*KMT2D*, *MLL2*)³³ syndrome, and most recently *SETD1A*-related disease (*KMT2F*)³⁴. The physiological functions of MLL proteins are yet to be fully characterized, however, the observation that mutations in different MLL genes cause phenotypically distinct syndromes (**Supplementary Table 6**) suggests that each MLL protein has a unique role regulating the expression of a specific set of genes^{35,36}.

487 Amongst the 4 reported *MLL*-gene disorders, dystonia appears unique to KMT2B-
488 related disease and is not described in other MLL syndromes (**Supplementary**
489 **Table 6**), providing further evidence that different MLL proteins mediate the
490 activation and transcription of a specific set of genes, with temporal and cellular
491 context³⁷. We utilized fibroblasts and CSF derived from patients to investigate
492 downstream effects of *KMT2B* mutations on specific gene expression. The rationale
493 for investigating *THAP1* and *TOR1A* in the first instance was based on a number of
494 factors, namely that (i) loss-of-function mutations in both genes cause progressive
495 generalized dystonia with cervical, oromandibular and laryngeal symptoms, similar
496 to those seen in KMT2B-dystonia^{38,39,40}, (ii) both genes are expressed in fibroblasts,
497 facilitating investigation in patient-derived tissue, (iii) analysis of methylation profiles
498 using ENCODE demonstrates a sharp H3K4me3 peak at the 5' region of both
499 *THAP1* and *TOR1A* in a wide range of cell types, including brain cells
500 (**Supplementary Fig. 7**), (iv) on human brain expression profiles, *THAP1* and
501 *KMT2B* similarly display highest expression in the cerebellum (**Fig 5b**,
502 **Supplementary Fig. 8**). We detected statistically significant reduced levels of
503 *THAP1* and *TOR1A* gene expression and THAP1 protein expression in patient
504 fibroblasts. The mechanisms causing such alterations in KMT2B-dystonia remain
505 yet to be elucidated. Whilst H3K4 methylation is clearly associated with the process
506 of active transcription, several studies have shown that H3K4 methylation is
507 required, not for absolute transcriptional output, but rather for transcription stability
508 or consistency⁴¹. Recent studies have suggested that H3K4Me is required to
509 minimize transcriptional variability between cells in a population, rather than
510 absolute expression^{41,42}, so the effects of *KMT2B* haploinsufficiency on
511 *THAP1/TOR1A* levels could conceivably operate via an intermediary sensitive to

stochastic fluctuations. Whilst our study focuses on two genes, it is highly likely that dysregulation of other genes and proteins are also involved in the disease pathophysiology of KMT2B-dystonia. Further studies will determine whether expression profiles of other genes are affected in KMT2B-dystonia and contributory to the phenotype.

CSF analysis is increasingly recognized as a highly useful tool for studying synaptic proteins and dysregulation of the dopaminergic system⁴³. In our study, CSF immunoblotting studies revealed significant reduction of D2R protein and increase in TH levels in patients with KMT2B-dystonia when compared to control CSF samples. Downregulation of D2R could conceivably impair post-synaptic activation of coupled G-proteins with subsequent downstream effects, as seen in other inherited dystonias. Reduced D2R striatal availability is reported in patients with DYT1 and DYT6 dystonia^{44,45}. Furthermore, D2R dysfunction is described in murine DYT1 models, where aberrant D2R-mediated responses are associated with reduced D2R protein levels and impaired G-protein activation⁴⁶. The observed rise in CSF TH levels could be secondary to reduced pre-synaptic D2 autoreceptors⁴⁷, which could conceivably impact dopamine synthesis and bioavailability. Interestingly patients with KMT2B-dystonia had normal CSF levels of the stable dopamine metabolite, homovanillic acid (HVA), indicating normal dopamine turnover (conversion of dopamine to HVA by monoamine oxidase and catechol-o-methyl transferase). Whilst CSF HVA levels accurately reflect dopamine turnover, they are not always a true indicator of dopamine synthesis and bioavailability. Low CSF HVA levels often correlate with low dopamine levels in patients with inherited disorders of dopamine deficiency such as TH deficiency, aromatic l-amino acid decarboxylase deficiency, and many inherited pterin defects³. However HVA levels

may also be normal (autosomal dominant GTP cyclohydrolase deficiency) or elevated (Dopamine Transporter Deficiency Syndrome) in diseases known to be associated with dopamine deficiency^{3,48}. Normal HVA levels in KMT2B-dystonia may therefore not reflect true dopamine levels. Indeed, the effect of *KMT2B* mutations on dopamine synthesis and bioavailability remain yet to be fully elucidated.

In conclusion, we report *KMT2B* mutations in 27 patients with a clinically recognizable, distinct form of dystonia. To date, the underlying etiology is only genetically resolved in a minority of childhood-onset cases of dystonia, which precludes confirmatory diagnosis, accurate disease prognostication and selection of appropriate treatment strategies. We have shown that many patients with molecular confirmation of KMT2B-dystonia have significant, sustained clinical improvement with DBS and referral for DBS assessment should thus be considered for this group of individuals. Identification of additional cases will allow further characterization of the full phenotypic disease spectrum. Our report highlights mutations in *KMT2B* as a new and important cause of early-onset dystonia, emphasizing the crucial role of KMT2B in the control of normal voluntary movement.

References

1. Charlesworth, G., Bhatia, K.P. & Wood, N.W. The genetics of dystonia: new twists in an old tale. *Brain* **136**, 2017-2037 (2013).
2. Albanese, A. *et al.* Phenomenology and classification of dystonia: a consensus update. *Mov. Disord.* **28**, 863-873 (2013).
3. Ng, J., Papandreou, A., Heales, S.J. & Kurian, M.A. Monoamine Neurotransmitter Disorders – clinical advances and future perspectives. *Nat. Rev. Neurol.* **11**, 567-584 (2015).
4. Fuchs, T. *et al.* Mutations in GNAL cause primary torsion dystonia. *Nat. Genet.* **45**, 88-92 (2013).
5. Karimi, M. & Perlmuter J.S. The role of dopamine and dopaminergic pathways in dystonia: insights from neuroimaging. *Tremor Other Hyperkinet. Mov.* **5**, 280 (2015).
6. Lin, J.P., Lumsden, D.E., Gimeno, H. & Kaminska, M. The impact and prognosis for dystonia in childhood including dystonic cerebral palsy: a clinical and demographic tertiary cohort study. *J. Neurol. Neurosurg. Psychiatry* **85**, 1239-1244 (2014).
7. Dale, R.C., Grattan-Smith, P., Nicholson, M. & Peters, G.B. Microdeletions detected using chromosome microarray in children with suspected genetic movement disorders: a single-centre study. *Dev. Med. Child Neurol.* **54**, 618-623 (2012).
8. Lek, M. *et al.* Analysis of protein-coding genetic variation in 60,706 humans. bioRxiv [Internet]; Available from: <http://biorxiv.org/content/early/2015/10/30/030338.abstract> (2015).
9. Kircher, M. *et al.* A general framework for estimating the relative

- pathogenicity of human genetic variants. *Nat. Genet.* **46**, 310-315 (2014).
10. Laimer, J., Hofer, H., Fritz, M., Wegenkittl, S. & Lackner, P. MAESTRO--
multi agent stability prediction upon point mutations. *BMC Bioinformatics* **16**,
116 (2015).
11. Pires, D.E., Ascher, D.B. & Blundell, T.L. DUET: a server for predicting
effects of mutations on protein stability using an integrated computational
approach. *Nucleic Acids Res.* **42**, W314-319 (2014).
12. Liu, Z. *et al.* Structural and functional insights into the human Borjeson-
Forssman-Lehmann syndrome-associated protein PHF6. *J. Biol. Chem.* **289**,
10069-10083 (2014).
13. Musselman, C.A. & Kutateladze, T.G. Handpicking epigenetic marks with
PHD fingers. *Nucleic Acids Res.* **39**, 9061-9071 (2011).
14. Sanchez, R. & Zhou, M.M. The PHD finger: a versatile epigenome reader.
Trends Biochem. Sci. **36**, 364-372 (2011).
15. Hsieh, J.J., Ernst, P., Erdjument-Bromage, H., Tempst, P. & Korsmeyer, S.J.
Proteolytic cleavage of MLL generates a complex of N- and C-terminal
fragments that confers protein stability and subnuclear localization. *Mol. Cell.*
Biol. **23**, 186-194 (2003).
16. Pless, B. *et al.* The heterodimerization domains of MLL-FYRN and FYRC--
are potential target structures in t(4;11) leukemia. *Leukemia* **25**, 663-670
(2011).
17. Wysocka, J. *et al.* WDR5 associates with histone H3 methylated at K4 and is
essential for H3 K4 methylation and vertebrate development. *Cell* **121**, 859-
872 (2005).
18. Song, J.J. & Kingston, R.E. WDR5 interacts with mixed lineage leukemia

- 604 (MLL) protein via the histone H3-binding pocket. *J. Biol. Chem.* **283**, 35258-
605 35264 (2008).
- 606 19.Chubb, J.R. *et al.* Developmental timing in Dictyostelium is regulated by the
607 Set1 histone methyltransferase. *Dev. Biol.* **292**, 519-532 (2006).
- 608 20.Malan, V. *et al.* 19q13. 11 deletion syndrome: a novel clinically recognisable
609 genetic condition identified by array comparative genomic hybridisation. *J.*
610 *Med. Genet.* **46**, 635-664 (2009).
- 611 21.Kruer, M.C. *et al.* Neuroimaging features of neurodegeneration with brain
612 iron accumulation. *AJNR Am. J. Neuroradiol.* **33**, 407-414 (2012).
- 613 22.Meyer, E., Kurian, M.A. & Hayflick, S.J. Neurodegeneration with Brain Iron
614 Accumulation: Genetic Diversity and Pathophysiological Mechanisms. *Annu.*
615 *Rev. Genomics Hum. Genet.* **16**, 257-279 (2015).
- 616 23.Ozelius, L. *et al.* SourceGeneReviews® [Internet]. Seattle (WA): University of
617 Washington, Seattle; [updated 2014 Jan 02] (1993-2016).
- 618 24.Klein, C. *et al.* SourceGeneReviews® [Internet]. Seattle (WA): University of
619 Washington, Seattle; [updated 2014 May 1] (1993-2016).
- 620 25.Kouzarides, T. Chromatin modifications and their function. *Cell* **128**, 693-705
621 (2007).
- 622 26.Black, J.C., Van Rechem, C. & Whetstone, J.R. Histone lysine methylation
623 dynamics: establishment, regulation, and biological impact. *Mol. Cell* **48**,
624 491-507 (2012).
- 625 27.Creyghton, M.P. *et al.* Histone H3K27ac separates active from poised
626 enhancers and predicts developmental state. *Proc. Natl. Acad. Sci. U S A*
627 **107**, 21931-21936 (2010).
- 628 28.Wang, Y., Li, X. & Hu, H. H3K4me2 reliably defines transcription factor

- binding regions in different cells. *Genomics* **103**, 222-228 (2014).
29. Shao, G.B. *et al.* Dynamic patterns of histone H3 lysine 4 methyltransferases and demethylases during mouse preimplantation development. *In Vitro Cell Dev. Biol. Anim.* **50**, 603-613 (2014).
30. Shen, E., Shulha, H., Weng, Z. & Akbarian, S. Regulation of histone H3K4 methylation in brain development and disease. *Philos. Trans. R. Soc. Lond. B. Biol. Sci.* **369** (2014).
31. Jones, W.D. *et al.* De novo mutations in MLL cause Wiedemann-Steiner syndrome. *Am. J. Hum. Genet.* **91**, 358-364 (2012).
32. Kleefstra, T. *et al.* Disruption of an EHMT1-associated chromatin-modification module causes intellectual disability. *Am. J. Hum. Genet.* **91**, 73-82 (2012).
33. Ng, S.B. *et al.* Exome sequencing identifies MLL2 mutations as a cause of Kabuki syndrome. *Nat. Genet.* **42**, 790-793 (2010).
34. Singh, T. *et al.* Rare loss-of-function variants in SETD1A are associated with schizophrenia and developmental disorders. *Nat. Neurosci.* **19**, 571-577 (2016).
35. Micale, L. *et al.* Molecular analysis, pathogenic mechanisms, and readthrough therapy on a large cohort of Kabuki syndrome patients. *Hum. Mutat.* **35**, 841-850 (2014).
36. Ang, S.Y. *et al.* KMT2D regulates specific programs in heart development via histone H3 lysine 4 di-methylation. *Development* **143**, 810-821 (2016).
37. Jakovcevski, M. *et al.* Neuronal Kmt2a/Mll1 histone methyltransferase is essential for prefrontal synaptic plasticity and working memory. *J. Neurosci.* **35**, 5097-5108 (2015).

-
38. Ozelius, L.J. *et al.* The early-onset torsion dystonia gene (DYT1) encodes an ATP-binding protein. *Nat. Genet.* **17**, 40-48 (1997).
39. Fuchs, T. *et al.* Mutations in the THAP1 gene are responsible for DYT6 primary torsion dystonia. *Nat. Genet.* **41**, 286-288 (2009).
40. Bressman, S.B. *et al.* Mutations in THAP1 (DYT6) in early-onset dystonia: a genetic screening study. *Lancet Neurol.* **8**, 441-446 (2009).
41. Benayoun BA, *et al.* H3K4me3 breadth is linked to cell identity and transcriptional consistency. *Cell* **158**, 673-688 (2014).
42. Muramoto, T., Müller, I., Thomas, G. Melvin, A. & Chubb, J.R. Methylation of H3K4 is required for inheritance of active transcriptional states. *Curr Biol.* **20**, 397-406 (2010).
43. Orteza, C. *et al.* Cerebrospinal fluid synaptic proteins as useful biomarkers in tyrosine hydroxylase deficiency. *Mol. Genet. Metab.* **114**, 34-40 (2015).
44. Carbon, M. *et al.* Abnormal striatal and thalamic dopamine neurotransmission: genotype-related features of dystonia. *Neurology* **72**, 2097-2103 (2009).
45. Asanuma, K. *et al.* Decreased striatal D2 receptor binding in non-manifesting carriers of the DYT1 dystonia mutation. *Neurology* **64**, 347-349 (2005).
46. Napolitano, F. *et al.* Dopamine D2 receptor dysfunction is rescued by adenosine A2A receptor antagonism in a model of DYT1 dystonia. *Neurobiol. Dis.* **38**, 434-445 (2010).
47. Lindgren, N., *et al.* Dopamine D(2) receptors regulate tyrosine hydroxylase activity and phosphorylation at Ser40 in rat striatum. *Eur. J. Neurosci.* **13**, 773-780 (2001).

-
- 678 48. Wijemanne, S. & Jankovic, J. Dopa-responsive dystonia--clinical and genetic
679 heterogeneity. *Nat. Rev. Neurol.* **11**, 414-424 (2015).
- 680 49. Trabzuni, D. *et al.* Quality control parameters on a large dataset of regionally
681 dissected human control brains for whole genome expression studies. *J.*
682 *Neurochem.* **119**, 275-282 (2011).

Acknowledgements

We would like to thank all our patients and their families for taking part in this study and encouraging international collaboration to seek out similar cases. Thank you to Dr Karin Tuschl for kindly providing the human cDNA panel, Miho Ishida for kindly providing the fetal cDNA and Dr Lorenzo Bassioni for kindly selecting DaTSCAN images for the Supplementary manuscript. MAK has a Wellcome Intermediate Clinical Fellowship. EM and MAK received funding from Gracious Heart Charity, Rosetrees Trust and Great Ormond Street Hospital Children's Charity. This research was supported by the National Institute for Health Research Biomedical Research Centre at Great Ormond Street Hospital for Children NHS Foundation Trust, University College London, and University of Cambridge and from the NIHR for the Bioresource for Rare Diseases (grant number RG65966). This study makes use of data generated by the DECIPHER community. A full list of centres who contributed to the generation of the data is available from <http://decipher.sanger.ac.uk> and via email from decipher@sanger.ac.uk Funding for the project was provided by the Wellcome Trust for UK10K (WT091310) and DDD Study. The DDD study presents independent research commissioned by the Health Innovation Challenge Fund [grant number HICF-1009-003] see Nature 2015;519:223-8 or www.ddduk.org/access.html for full acknowledgement. AP has a joint Action Medical Research/ British Paediatric Neurology Association Research Training Fellowship and receives funding from the NBIA Disorders Association and Child Brain Research. DA is supported by the Prusiner-Abramsky Award. KJP has an Academy of Medical Sciences Clinical Starter Grant. BPD received funding from grants 20143130-La Marató de TV3 and PI15/00287-Ministerio Español de Economía y Competitividad. JPL has been supported by a Guy's and St Thomas

708 Charity New Services and Innovation Grant: G060708; The Dystonia Society (UK):

709 Grants 01/2011 and 07/2013 and an Action Medical Research: AMR - GN2097.

710

711 **Disclosures**

712 HP has unrestricted support for Educational Activity from Medtronic.

713

714 **Figure 1**

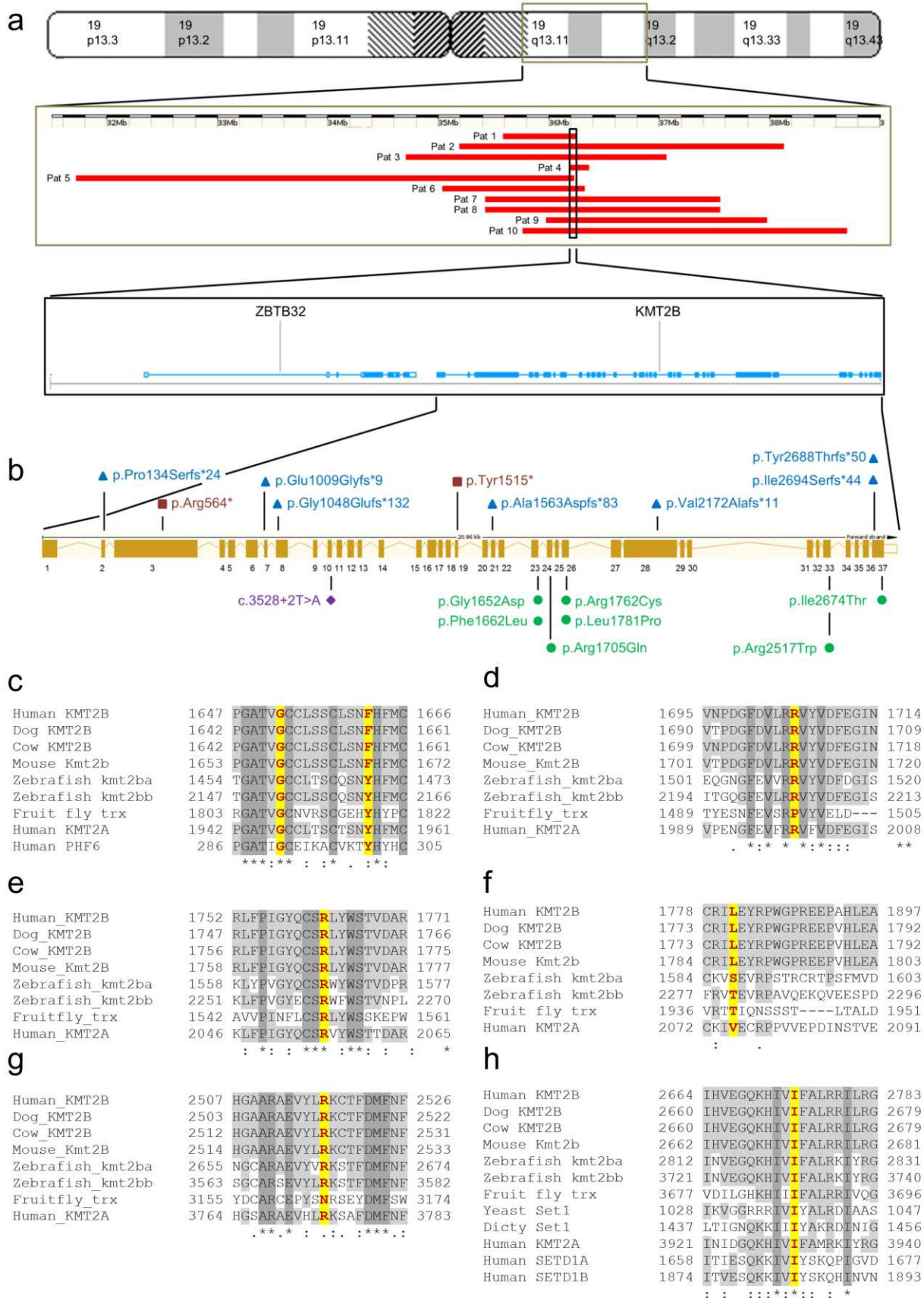


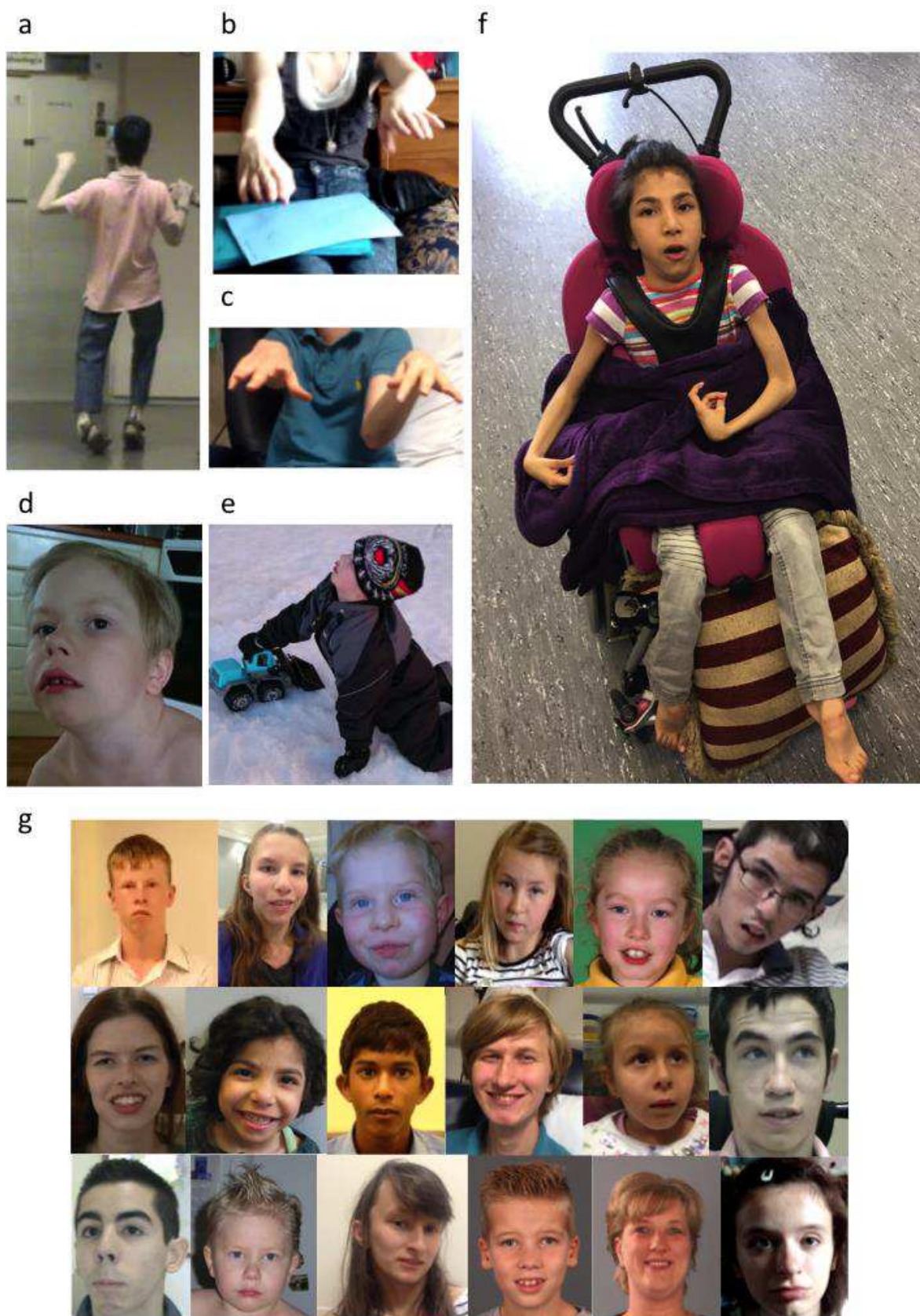
Figure 1:

Molecular Genetics Findings in Patients with *KMT2B* Mutations

(a) Top panel: Schematic representation of chromosome 19. Middle panel: Ten microdeletions on 19q13.11-19q13.12 are displayed as horizontal red bars (GRCh37/Hg19). Lower panel: The smallest overlapping region comprises two genes, *ZBTB32* and *KMT2B*. **(b)** Schematic of exon-intron structure of *KMT2B* (based on NCBI Reference Sequence: NM_014727.2) is shown indicating the location of the 7 frameshift insertions and deletions (blue, above gene), 2 stop-gain mutations (dark red, above gene), 1 splice site variant (purple, below gene) and 7 missense changes (in green, below gene). **(c)** Alignment of *KMT2B* amino acid sequences from seven different species, the human paralog *KMT2A* (another member of the MLL protein family) and the human PHF6 protein used to model the PHD-like domain. Gly1652 (in red) is highly conserved in all listed amino acid sequences, while the Phe1662 residue (in red) is either conserved or tolerates replacement by the similar amino acid, Tyr without predicted functional effect (**Supplementary Fig. 10**). **(d-g)** Alignment of *KMT2B* amino acid sequences from seven different species and the human paralog *KMT2A*. **(d)** Arg1705 (in red) is conserved to zebrafish and in human *KMT2A*. **(e)** Arg1762 is fully conserved throughout species. **(f)** Leu1781 (in red) is conserved in all listed mammalian homologs of *KMT2B*. **(g)** Arg2517 (in red) is conserved to zebrafish and in human *KMT2A*. **(h)** Alignment of *KMT2B* amino acid sequences from seven different species, the human paralog *KMT2A* and SET domain containing proteins (human SETD1A/SETD1B, yeast Set1, *Dictyostelium discoideum* Set1. Ile2674 (in red) is highly conserved in all listed amino acid sequences. Residues matching human *KMT2B* (grey), not matching (white), amino acids conserved in all representative sequences (dark grey). * positions of fully conserved residues; :

742 conservation between groups of strongly similar properties and . conservation between
743 groups of weakly similar properties.

744 **Figure 2**



746

747 **Figure 2:**

748 **Clinical Features of Patients with *KMT2B* Mutations**

749 (a) Patient 17, age 13 years, evidence of gait disturbance with dystonic posturing of the
750 four limbs. (b) Patient 27, age 19 years and (c) Patient 14, age 18 years both showing
751 bilateral upper limb dystonic posturing. (d, e) Patient 23, age 8 years with retrocollis. (f)
752 Patient 12, age 6 years, generalized dystonia, with jaw-opening dystonia and 4-limb
753 posturing. (g) Montage of patient faces: Top row (left to right) Patients 1, 2, 3, 4, 8, 9;
754 Middle row (left to right) Patients 11, 12, 13, 14, 16, 17 and Bottom row (left to right)
755 Patients 21, 23, 25, 26a, 26b, 27. Facial elongation, broad nasal base and bulbous nasal
756 tip, particular evident in Patients 1, 2, 4, 9, 11, 12, 14, 17, 23, 25, 26a, 26b, 27.

757

Figure 3

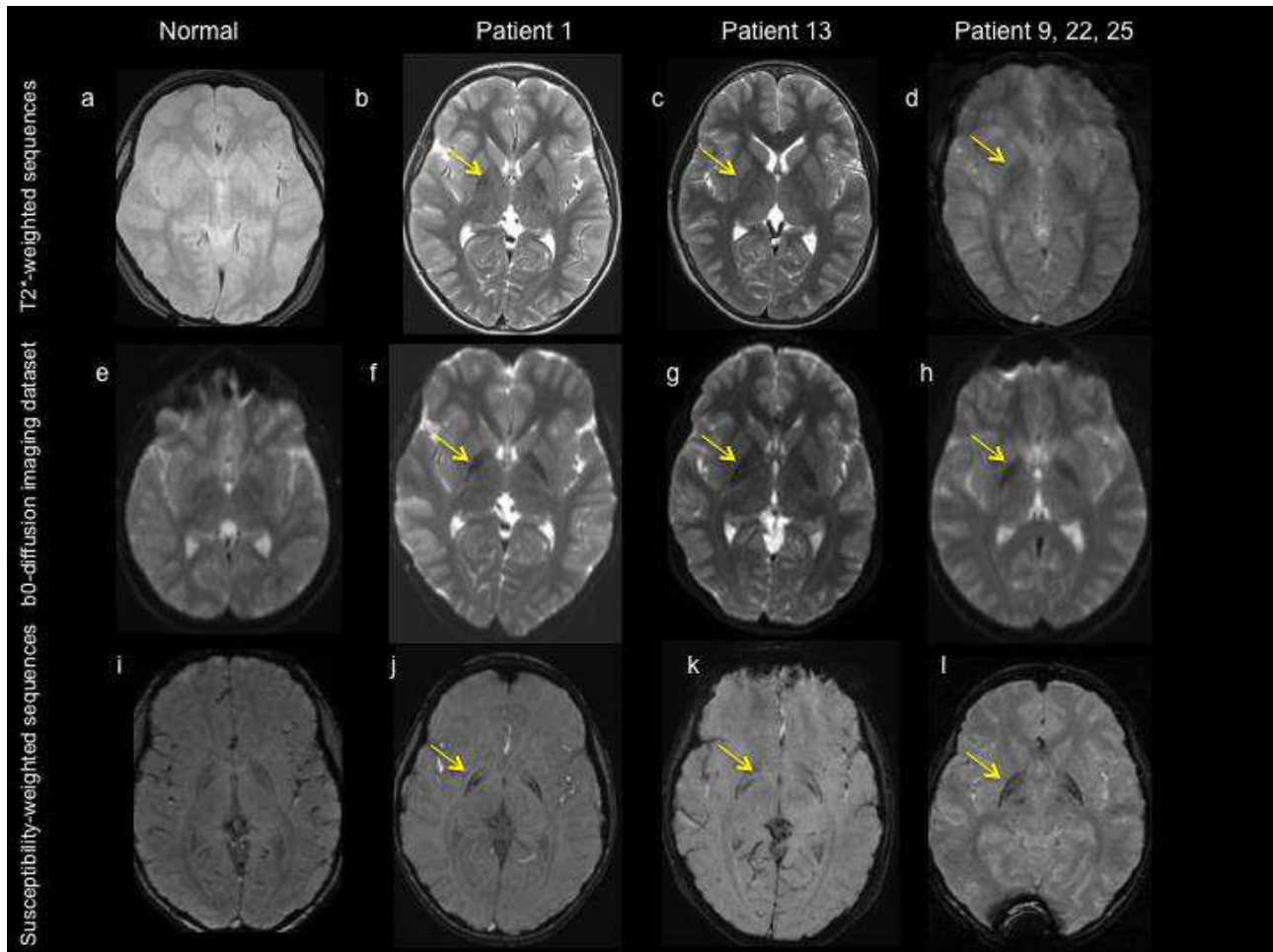


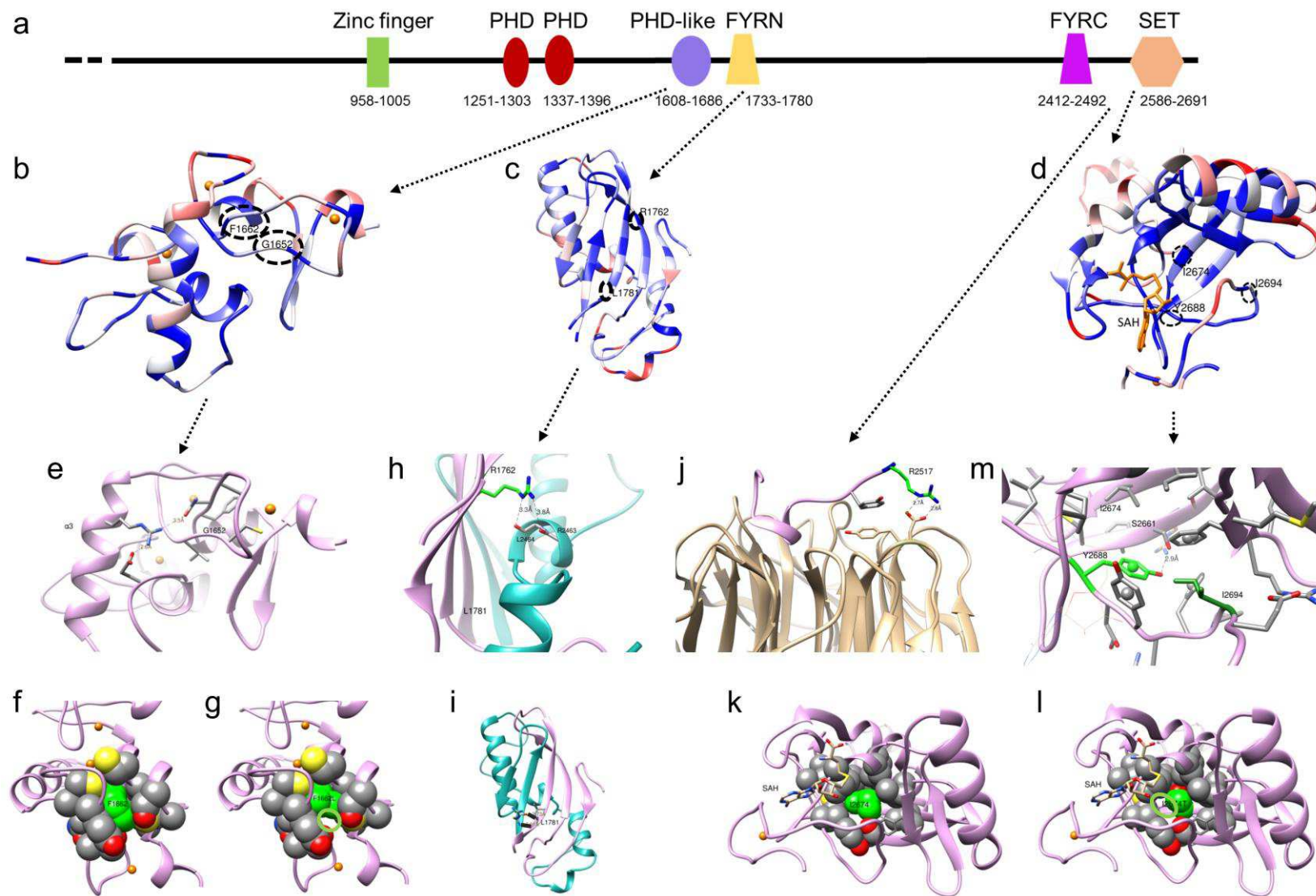
Figure 3:

Radiological Features in KMT2B-patients

Magnetic resonance imaging (MRI) with T2*-weighted sequences (**a-d**), diffusion- imaging datasets with b-value of zero (**e-h**) and susceptibility weighted sequences (**i-l**). Abnormal findings indicated by yellow arrows. (**a,e,i**) Representative MRI from control subjects for T2*-weighted sequences (**a**: age 10y2m), diffusion-weighted sequences (**e**: age 10y4m) and susceptibility weighted sequences (**i**: age 10y8m) indicating normal appearances of basal ganglia on all three sequences. (**b,f,j**) Patient 1, age 9y5m, (**c,g,k**) Patient 13, age 11y3m, (**d**) Patient 9, age 15y1m, (**h**) Patient 22 age 13y1m and (**l**) Patient 25, age 16y -

770 all show evidence of bilateral subtle hypointensity of the globus pallidus with hypointense
771 lateral streak of globus pallidus externa.

772 **Figure 4**

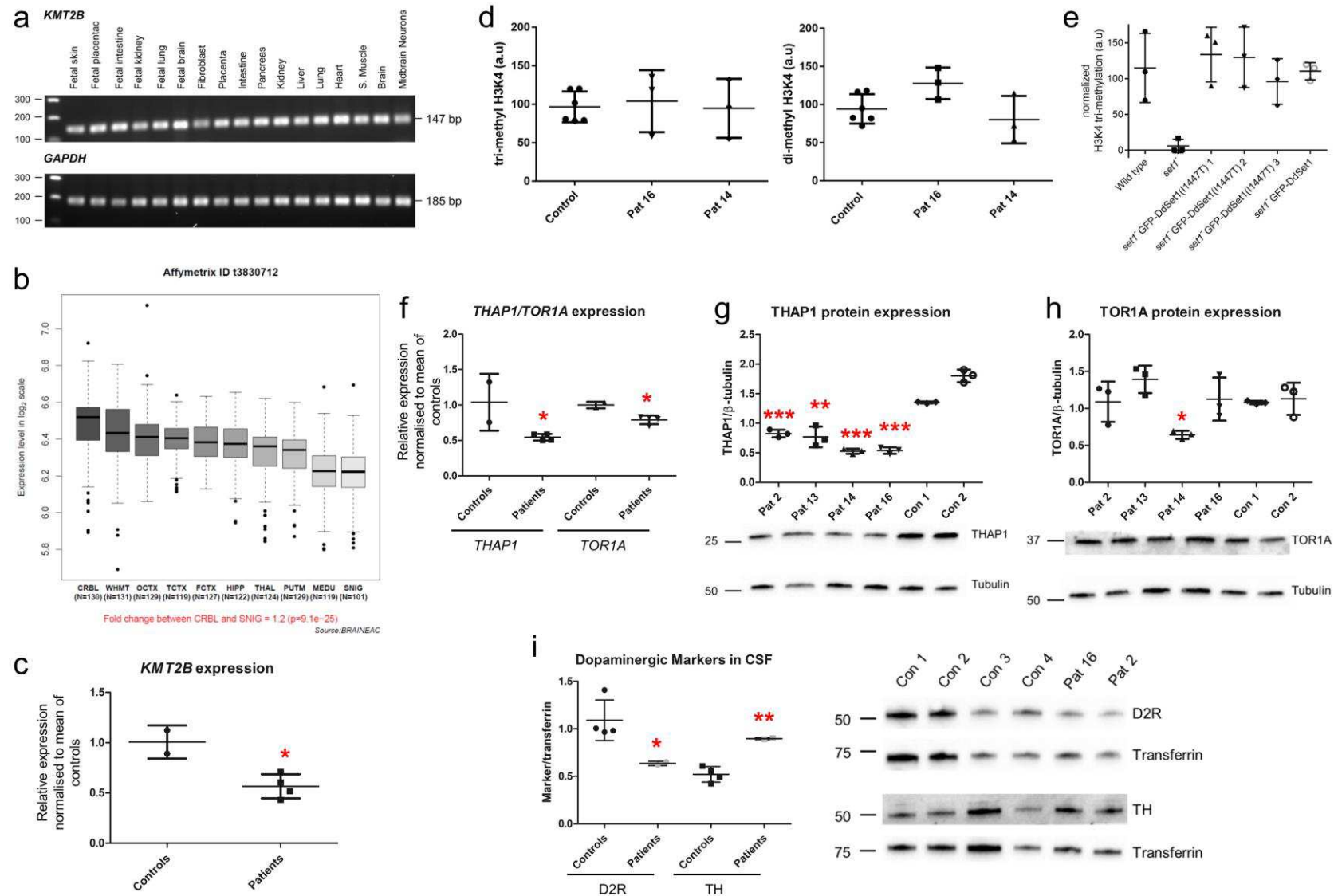


774 **Figure 4:**

775 **Homology Modelling of KMT2B Protein Structure**

776 (a) Schematic of domain architecture of KMT2B. (b-d) The degree of amino conservation
777 is displayed in the structural models for the different domains. Red to blue indicates
778 increasing conservation. (b) Model of PHD-like domain shows the mutation sites Gly1652
779 and Phe1662 (c) Model of the FYRN domain presents the position and conservation of
780 Arg1762 and Leu1781. (d) Model of the SET methyltransferase domain indicates the
781 position and conservation of Ile2674, Tyr2688 and Ile2694. (e) Location of Gly1652 in the
782 PHD-like domain model and the hydrogen bond network in the vicinity are shown. Helix $\alpha 3$
783 is also indicated. (f) Hydrophobic packing involving Phe1662 (green) is displayed. (g)
784 Change to leucine (green) at position 1662 is predicted to cause loss of contact within the
785 hydrophobic core. Residue side chains are presented as spheres highlighting van der
786 Waals contacts. (h) Interactions involving Arg1762 (green) from FYRN with Arg2463 and
787 Leu2464 of FYRC. The hydrogen bond interactions are highlighted. (i) Leu1781 shown at
788 the interface of FYRN (pink)/FYRC (blue) domains. The backbone hydrogen bonds
789 stabilizing the sheet structure are highlighted. (j) Interactions involving Arg2517 (green)
790 and WDR5 (brown). The salt bridge interaction between Arg2517 of KMT2B and Asp172
791 of WDR5 is highlighted. (k) Location and contacts involving Ile2674 (green) in the
792 hydrophobic core of the SET domain are exhibits. SAH is displayed in light brown. (l)
793 Conversion to threonine (green) at position 2674 is predicted to result in loss of contacts in
794 the core. (m) Interactions involving Tyr2688 (light green) and Ile2694 (dark green) in the
795 core of the SET domain. The hydrogen bond between Tyr2688 and Ser2661 is
796 highlighted.

Figure 5



799 **Figure 5:**

800 **Functional Investigation of the Downstream Effects of Mutations in *KMT2B***

801 (a) PCR analysis of human fetal and adult cDNA for expression of *KMT2B*. *KMT2B* is
802 widely expressed in a range of human tissues, including fibroblasts, brain tissue and
803 midbrain dopaminergic neurons. (b) Box plots of *KMT2B* mRNA expression levels in 10
804 adult brain regions (source: BRAINEAC; <http://www.braineac.org/>). The expression levels
805 are based on exon array experiments as previously described and are plotted on a log2
806 scale (y axis)⁴⁹. This plot shows that *KMT2B* is ubiquitously expressed across all 10 brain
807 regions analyzed, with expression higher in the cerebellum than in any other region.
808 Putamen (PUTM), frontal cortex (FCTX), temporal cortex (TCTX), occipital cortex (OCTX).
809 hippocampus (HIPPO), substantia nigra (SNIG), medulla (specifically inferior olivary
810 nucleus, MEDU), intralobular white matter (WHMT), thalamus (THAL), and cerebellar
811 cortex (CRBL). “N” indicates the number of brain samples analyzed to generate the results
812 for each brain region. Whiskers extend from the box to 1.53 the interquartile range. (c)
813 Quantitative RT-PCR indicates that patients with *KMT2B* mutations (n=4) have
814 significantly decreased fibroblast mRNA levels of *KMT2B* when compared to controls
815 (Controls = $1.01 \pm 0.16SD$, n=3 technical replicates of 2 biological samples; Patients =
816 $0.57 \pm 0.12SD$, n=3 technical replicates of 4 biological samples; two-tailed unpaired t-test,
817 p-value 0.0182). (d) Quantification of immunoblotting of tri-methyl H3K4 (left) and di-
818 methyl H3K4 (right) in histones extracted from patient-derived fibroblasts (Patient 14 and
819 16), and two control fibroblast cell lines. Methylation values are normalized to pan-histone
820 H3 levels. Individual data-points are plotted with center bar showing mean and error bars
821 showing standard deviation. Differences between control and patient-derived samples are
822 not significant (H3K4me3: Controls = $96.63 \pm 19.98SD$; Patient 16 = $104.1 \pm 40.31SD$;
823 Patient 14 = $94.75 \pm 38.36SD$; p=0.62; H3K4me2: Controls = $94.33 \pm 19.25SD$; Patient 16 =
824 $127.8 \pm 20.79SD$; Patient 14 = $80.23 \pm 31.09SD$; p=0.07). n=3 fibroblast samples (technical

825 replicates). (e) Quantification of immunoblotting of tri-methyl H3K4 in *Dictyostelium* cell
826 lysates. Tri-methyl H3K4 intensity values are normalized against levels of total histone H3.
827 H3K4 tri-methylation is impaired in set1- cells compared to wild type. Expression of GFP-
828 DdSet1 or GFP-DdSet1(Ile1447Thr) in set1- cells rescues levels of H3K4Me3. Individual
829 data-points are plotted with center bar showing mean and error bars showing standard
830 deviation (Wild type = $115 \pm 48.25SD$; set1- = $5.94 \pm 9.37SD$; set1- GFP-DdSet1(I1447T) 1 =
831 $133.7 \pm 38.11SD$; set1- GFP-DdSet1(I1447T) 2 = $129.8 \pm 42.34SD$; set1- GFP-
832 DdSet1(I1447T) 3 = $96.07 \pm 31.82SD$; set1- GFP-DdSet1 = $110.5 \pm 12.02SD$). n=3 samples
833 (technical replicates). (f) Quantitative RT-PCR of *THAP1* and *TOR1A*, indicates that
834 patients have a reduction of *THAP1*, and to a lesser extent of *TOR1A* transcripts in
835 comparison to controls (*THAP1*: Controls = $1.04 \pm 0.40SD$, n=3 technical replicates of 2
836 biological samples; Patients = $0.55 \pm 0.05SD$, n=3 technical replicates of 4 biological
837 samples; two-tailed unpaired t-test, p-value 0.0498; *TOR1A*: Controls = $1.00 \pm 0.05SD$, n=3
838 technical replicates of 2 biological samples; Patients = $0.79 \pm 0.06SD$, n=3 technical
839 replicates of 4 biological samples; two-tailed unpaired t-test, p-value 0.0140). (g)
840 Immunoblotting studies in fibroblasts indicate a significant reduction in THAP1 for Patient
841 2, 13, 14 and 16 when compared to controls (Control 1 = $1.34 \pm 0.02SD$; Control 2 = $1.80 \pm$
842 $0.11SD$; Patient 2 = $0.83 \pm 0.06SD$; Patient 13 = $0.77 \pm 0.17SD$; Patient 14 = $0.53 \pm 0.04SD$;
843 Patient 16 = $0.54 \pm 0.06SD$; Kruskal-Wallis test, p-value 0.0078). n=3 fibroblast protein
844 samples (technical replicates). (h) Immunoblotting studies in fibroblasts indicate a
845 statistically reduced level of TOR1A in Patient 14 when compared to controls (Control 1 =
846 $1.08 \pm 0.02SD$; Control 2 = $1.13 \pm 0.22SD$; Patient 14 = $0.64 \pm 0.05SD$; two-tailed unpaired t-
847 test, p-value 0.0196), but not for Patient 2, 13 and 16 (Patient 2 = $1.09 \pm 0.27SD$; Patient 13
848 = $1.39 \pm 0.18SD$; Patient 16 = $1.13 \pm 0.29SD$; Kruskal-Wallis test, p-value 0.0812). n=3
849 fibroblast protein samples (technical replicates). (i) CSF immunoblotting studies on Patient

850 2 and 16 show markedly reduced levels of D2R and increased levels of TH when
851 compared to control CSF (D2R: Controls = 1.09 ± 0.21 SD, n=4 control CSF samples
852 (biological replicates); Patients = 0.64 ± 0.02 SD, n=2 patient CSF samples (biological
853 replicates); two-tailed unpaired t-test, p-value 0.0471; TH: Controls = 0.52 ± 0.08 SD, n=4
854 control CSF samples (biological replicates); Patients = 0.90 ± 0.01 SD, n=2 patient CSF
855 samples (biological replicates); two-tailed unpaired t-test, p-value 0.0036).

Table 1a: *KMT2B* Mutations and Evolution of Motor Phenotype in KMT2B-dystonia

Pat	Age (y)	<i>KMT2B</i> mutation ⁽¹⁾	Symptoms at presentation: Body distribution & motor features	Onset of dystonia (y)	Bilateral LL involvement (y)	Bilateral UL involvement (y)	Onset of cranial, cervical, laryngeal dystonia (y)	Symptoms of cranial, cervical, laryngeal dystonia	Trial of medication and clinical response	Deep brain stimulation (DBS)
1	14 M	Deletion: Chr19: 35,608,666-36,233,508	RLL Right foot posturing Gait disturbance	4	6	6-11	5	Dysarthria Dysphonia Swallowing difficulties	L-dopa trial – no benefit	No
2	14 F	Deletion: Chr19: 35,197,252-38,140,100	Bilateral LL Limping Gait disturbance	7	7	8-11	8	Dysarthria Dysphonia Drooling	L-dopa trial – no benefit BLF – no benefit	No
3	9 M	Deletion: Chr19: 34,697,740-37,084,510	RLL Right foot posturing Gait disturbance	2.5	3	6-7	4	Dysarthria Dysphonia Swallowing difficulties Drooling	GBP – some reduction in tone	No
4	11 F	Deletion: Chr19: 36,191,100-36,376,860	LLL Left toe walking Gait disturbance	4	8	9-12 m	5	Dysarthria Dysphonia Swallowing difficulties Drooling	L-dopa trial – minimal benefit THP – minimal benefit	Planned for 2016
5	20 M	Deletion: Chr19: 31,725,360-36,229,548	Developmental delay Gait disturbance	Present but age of onset not known	Present but age of onset not known	Present but age of onset not known	Not known	Nasal voice	None	No
6	10 F	Deletion: Chr19: 35,017,972-36,307,788	RLL Right foot inversion	2.5	4	4	4-7	Dysarthria/Anarthria Jaw-opening dystonia Swallowing difficulties NGF 6y PEG 8y Torticollis Severe retrocollis	L-dopa trial – no benefit THP – no benefit	Inserted age 7y Sustained excellent clinical benefits 3y post-DBS, marked improvement in torticollis, retrocollis, manual abilities and left leg dystonia. Loss of efficacy when 'DBS off' for almost a year and functional recovery when switched on again.
7	21 M	Deletion: Chr19: 35,414,997-37,579,142	RLL Right foot dragging Gait disturbance	7	7-8	13	13	Dysarthria Dysphonia Swallowing difficulties	L-dopa trial – no benefit BLF – no benefit	No

358

Pat	Age (y)	KMT2B mutation ⁽¹⁾	Symptoms at presentation: Body distribution & motor features	Onset of dystonia (y)	Bilateral LL involvement (y)	Bilateral UL involvement (y)	Onset of cranial, cervical, laryngeal dystonia (y)	Symptoms of cranial, cervical, laryngeal dystonia	Trial of medication and clinical response	Deep brain stimulation (DBS)
8	17 F	Deletion: Chr19: 35,414,997-37,579,142	RLL Right foot posturing	4	6	4-12	2.5	Dysarthria Dysphonia Drooling Torticollis	L-dopa trial – no benefit	Inserted age 10y Good response over 6 years, particularly evident after replacement of faulty right DBS lead
9	14 M	Deletion: Chr19: 35,967,904-37,928,373	Bilateral LL Gait disturbance	4	4	9-13	9	Dysarthria Dysphonia	L-dopa trial – possible initial benefit but not sustained	Inserted age 14y Very good clinical response at 4m post DBS with restoration of independent ambulation
10	7 F	Deletion: Chr19: 35,794,775-38,765,822	Bilateral LL Intermittent toe walking Gait disturbance	4	4	-	-	-	None	No
11	25 F	c.399_400insT p.Pro134Serfs*24	RUL Right Hand Cramps and Posturing	6	12	12	14 ⁽²⁾	Anarthria Orolingual dystonia Tongue thrusting Swallowing difficulties PEG	L-dopa trial – poorly tolerated, no benefit	Being considered
12	6 F	c.1690C>T p.Arg564*	Bilateral LL Toe walking	4	5	6	5	Dysarthria Swallowing difficulties	L-dopa trial – no benefit	No
13	11 M	c.3026_3027del p.Glu1009Glyfs*9	Bilateral UL Posturing, tremor Difficulty handwriting	8	9-10	8	9	Dysarthria Dysphonia	L-dopa trial – no benefit	No
14	18 M	c.3143_3149del p.Gly1048Glyfs*132	Bilateral UL Posturing of hands Myoclonic jerks	8	13	8	13	Dysarthria Dysphonia Swallowing difficulties	L-dopa trial – no benefit	No
15	20 F	c.4545C>A p.Tyr1515*	Bilateral LL Toe Walking Clumsy	2	9	9	8.5	Dysarthria Dysphonia Oromandibular dystonia Swallowing difficulties PEG 18y	Moderate responses to (and currently taking) THP CLZ L-dopa BLF	No

359

Pat	Age (y)	KMT2B mutation ⁽¹⁾	Symptoms at presentation: Body distribution & motor features	Onset of dystonia (y)	Bilateral LL involvement (y)	Bilateral UL involvement (y)	Onset of cranial, cervical, laryngeal dystonia (y)	Symptoms of cranial, cervical, laryngeal dystonia	Trial of medication and clinical response	Deep brain stimulation (DBS)
	Sex M/F									
16	6 F	c.4688del p.Ala1563Aspfs*83	Bilateral LL Increasing falls Gait disturbance	3	3	5	6	Dysarthria Dysphonia	L-dopa trial – no benefit THP – initial benefit, not sustained	No
17	17 M	c.6515_6518delins p.Val2172Alafs*11.	Bilateral LL Toe walking Gait disturbance	1	1	8	12	Dysarthria Dysphonia Swallowing difficulties	L-dopa trial – no benefit TBZ – no benefit BLF and THP – mild benefit	Inserted age 16y Very good clinical response 4m post-DBS with restoration of independent ambulation
18	20 F	c.8061del p.Tyr2688Thrfs*50	Clumsy movements Difficulties with speech articulation	1	-	-	Infancy	Dysarthria Dysphonia Swallowing and chewing difficulties	No	No
19	28 M	c.8076del p.Ile2694Serfs*44	Bilateral LL Toe walking Severe speech delay	2	3	4 (L>R)	7	Anarthria Jaw opening dystonia Tongue protrusion Swallowing difficulties PEG 8y L torticollis, R laterocollis	L-dopa trial – no benefit THP and TBZ reduced tongue protrusion	Inserted age 27y Improvement of jaw opening dystonia and tongue protrusion
20	40 M	c.3528+2T>A	LLL Gait disturbance L foot dragging Clumsiness	4	5	8	10	Severe dysarthria Dysphonia L Torticollis	L-dopa trial – no benefit TBZ, THP, SUL – no benefit	Inserted age 32y – no benefit. Electrode replaced in 2009 with sustained improvement in foot posture but only transient benefit to cervical, UL and LL dystonia.
21	18 M	c.4955G>A p.Gly1652Asp	RLL Right leg posturing	6	8	12	5	Dysarthria Dysphonia Swallowing difficulties	L-dopa trial – no benefit THP – not tolerated	Inserted age 15y Sustained clinical benefit 3y post-DBS, improved dystonia and independent walking
22	20 F	c.4986C>A p.Phe1662Leu	RLL Right foot posturing Abnormal gait	5	8	5-13	5-6	Dysarthria Dysphonia Swallowing difficulties Torticollis	L-dopa trial – no benefit BLF – no benefit THP – low dose, mild benefit BTX neck – reduction in pain but no functional	Inserted age 20y Very good clinical response 9m post DBS with improved dystonia and independent walking

benefit										
Pat	Age (y)	KMT2B mutation ⁽¹⁾	Symptoms at presentation: Body distribution & motor features	Onset of dystonia (y)	Bilateral LL involvement (y)	Bilateral UL involvement (y)	Onset of cranial, cervical, laryngeal dystonia (y)	Symptoms of cranial, cervical, laryngeal dystonia	Trial of medication and clinical response	Deep brain stimulation (DBS)
23	8 M	c.5114G>A p.Arg1705Gln	Bilateral LL Toe-walking	3	3	6	6.5	Dysarthria Torticollis	L-dopa trial – no benefit CLZ, THP, IT BLF – some benefit	Inserted age 7y with considerable benefit
24	27 F	c.5284C>T p.Arg1762Cys	LLL Tiptoe walking and in-turning of L foot	6	6	7	7	Dysarthria Anarthria from 14-15y Reduced tongue movements Swallowing preserved	L-dopa trial – no benefit THP- no benefit	No
25	19 F	c.5342T>C p.Leu1781Pro	RLL Right foot posturing Gait disturbance	8	12	13	10	Dysarthria Dysphonia Swallowing difficulties Torticollis	L-dopa trial – no benefit LVT – mild benefit	Inserted age 19y Very good clinical response 4m post-DBS with improved dystonia and ambulation ⁽³⁾
26a	8 M	c.7549C>T p.Arg2517Trp	Delayed speech Delayed motor development	-	-	-	8	Severe paroxysmal retrocollis and jaw dystonia	-	No
26b	46 F	c.7549C>T p.Arg2517Trp	Bilateral UL UL posturing Torticollis Inability to walk long distances and run	23	26	23	23	Dysphonia Torticollis	None	No
27	19 F	c.8021T>C p.Ile2674Thr	RUL Posturing, tremor Difficulty handwriting Myoclonic jerks	9	11-13	10	9-10	Dysphonia	L-dopa trial – no benefit THP – no benefit LVT – no benefit CBZ – initial benefit, not sustained CLZ – not tolerated	No

BLF: baclofen; BTX: botulinum toxin; CLZ: clonazepam; GBP: gabapentin; IT: intrathecal; LL: lower limbs; LLL: left lower limb; LVT: levetiracetam; m: months; NGF: nasogastric feeding; Pat: patient; PEG: percutaneous endoscopic gastrostomy; RLL: right lower limb; RUL: right upper limb; SUL: sulpiride; UL: upper limbs; TBZ: tetrabenzine; THP: trihexyphenidyl; y: years

⁽¹⁾ based on NCBI Reference Sequence: NM_014727.2

⁽²⁾ onset shortly after being fitted with orthodontic braces

⁽³⁾ had undergone 2 posterior cranial fossa explorations and palatal surgery before DBS

367 **Table 1b: Additional Clinical Features in KMT2B-patients**

Patient	KMT2B mutation	Number of genes in microdeletion	Intellectual disability	Dysmorphic features	Additional neurological features	Psychiatric features	Abnormal skin features	Other systemic manifestations
1	Deletion: Chr19: 35,608,666-36,233,508	38	Mild	Elongated face	Not reported	Not reported	Not reported	Not reported
2	Deletion: Chr19: 35,197,252- 38,140,100	124	No	Elongated face Bulbous nasal tip	Not reported	Not reported	Not reported	Not reported
3	Deletion: Chr19: 34,697,740 -37,084,510	109	Moderate	Elongated face	Not reported	Not reported	Cutis aplasia ⁽¹⁾	Retinal dystrophy
4	Deletion: Chr19: 36,191,100-36,376,860	14	V mild - subtle memory problems	Elongated face Broad nasal bridge Bulbous nasal tip	Not reported	Prone to anxiety ⁽²⁾	Not reported	Not reported
5	Deletion: Chr19: 31,725,360-36,229,548	110	Moderate	Sparse hair Blepharophimosis Absent eyelashes of lower eyelids Low set, posteriorly rotated ears Epicanthic folds Narrow nasal bridge, ridge and point Largely bifid tongue Micrognathia Teeth overcrowding Finger contractures 5 th finger clinodactyly Toe over-riding Dysplastic toenails	Microcephaly	Not reported	Occipital cutis aplasia	Small echogenic kidneys with low GFR, required renal transplant at 17 years
6	Deletion: Chr19: 35,017,97-36,307,788	69	No	Not reported	Microcephaly	Not reported	Not reported	Not reported
7	Deletion: Chr19: 35,414,997-37,579,142	99	Mild	Elongated face	Absence seizures	Not reported	Not reported	Absent right testis
8	Deletion: Chr19: 35,414,997-37,579,142	99	Mild	5 th finger clinodactyly	Not reported	Not reported	Ectodermal dysplasia	Not reported
9	Deletion: Chr19: 35,967,904-37,928,373	79	Mild	Elongated face	Strabismus	Not reported	Not reported	Cleft palate
10	Deletion: Chr19: 35,794,775-38,765,822	111	Moderate	Not reported	Strabismus	Not reported	Not reported	Short stature Bronchiectasis

Patient	KMT2B mutation	Number of genes in microdeletion	Intellectual disability	Dysmorphic features	Additional neurological features	Psychiatric features	Abnormal skin features	Other systemic manifestations
11	c.399_400insT p.Pro134Serfs*24	-	No	Bulbous nasal tip	Not reported	Not reported	Not reported	Not reported
12	c.1690C>T p.Arg564*	-	Moderate	Elongated face Bulbous nasal tip, short nasal root, Hypertelorism, large mouth with full lower lip	Epilepsy	Not reported	Not reported	Not reported
13	c.3026_3027del p.Glu1009Glyfs*9	-	V mild - difficulties with attention	Elongated face	Not reported	Not reported	Not reported	Not reported
14	c.3143_3149del p.Gly1048Glufs*132	-	No	Elongated face Bulbous nasal tip	Not reported	Not reported	Not reported	Not reported
15	c.4545C>A p.Tyr1515*	-	No	Elongated face Bulbous nasal tip	Not reported	Not reported	Not reported	Not reported
16	c.4688del p.Ala1563Aspfs*83	-	No	Elongated face	Not reported	Not reported	Not reported	Not reported
17	c.6515_6518delins p.Val2172Alafs*11.	-	No	Elongated face	Not reported	Not reported	Phimosos	Short stature
18	c.8061del p.Tyr2688Thrfs*50	-	Mild	Micrognathia Atrophic tongue Bulbous nasal tip 5 th finger clinodactyly	Not reported	Not reported	Not reported	Not reported
19	c.8076del p.Ile2694Serfs*44	-	No	Short stature	Delay in saccade initiation and hypometric vertical saccades	ADHD ⁽³⁾ with no response to Ritalin	Not reported	Not reported
20	c.3528+2T>A	-	Moderate 6y- verbal IQ 74 Performance IQ 87 No cognitive decline	Not reported	Not reported	Not reported	Not reported	Not reported
21	c.4955G>A p.Gly1652Asp	-	Mild	Elongated face	Not reported	Not reported	Not reported	Short stature Hypertrichosis
22	c.4986C>A p.Phe1662Leu	-	No	Elongated face Bulbous nasal tip	Not reported	Not reported	Not reported	Not reported

Patient	KMT2B mutation	Number of genes in microdeletion	Intellectual disability	Dysmorphic features	Additional neurological features	Psychiatric features	Abnormal skin features	Other systemic manifestations
23	c.5114G>A p.Arg1705Gln	-	Mild-moderate 6y WISC-IV 50-60	Elongated face Bulbous nasal tip Broad philtrum, Upslanted eyes, epicanthus, low-set ears, periorbital fullness, gap between front teeth	Spasticity in lower limbs from 6y	Not reported	Ichthyotic skin lesions with criss-cross pattern under the feet and at knees, broad scarring after operation	Episodic vomiting
24	c.5284C>T p.Arg1762Cys	-	No	Short stature	Oculomotor apraxia with difficulty initiating saccades. Mild spasticity	No	Not reported	Not reported
25	c.5342T>C p.Leu1781Pro	-	No	Elongated face Bulbous nasal tip	Not reported	Not reported	Not reported	Not reported
26a	c.7549C>T p.Arg2517Trp	-	No	Bulbous nasal tip	None	ADHD ⁽³⁾ Currently on methylphenidate, oxazepam, risperidone	Not reported	Not reported
26b	c.7549C>T p.Arg2517Trp	-	No	Bulbous nasal tip	Idiopathic intracranial hypertension – on acetazolamide	None	Not reported	Not reported
27	c.8021T>C p.Ile2674Thr	-	V subtle mild learning difficulties	Bulbous nasal tip	Not reported	Anxiety Self-harm behavior Depression Obsessive- compulsive traits ⁽⁴⁾	Not reported	Not reported

(1) Supplementary Figure 3c

(2) Identified on formal psychology review

(3) Diagnosed by psychiatrist and under regular psychiatry review

(4) Under regular review with psychiatrist (ICD-10-CM F06.30; ICD-10-CM F42)

ADHD: attention deficit hyperactivity disorder; GFR: glomerular filtration rate; V: very; y: years